Published in final edited form as:
Nat Immunol. 2008 August ; 9(8): 847–856. doi:10.1038/ni.1631.

Silica crystals and aluminum salts mediate NALP-3 inflammasome activation via phagosomal destabilization

Veit Hornung[1,*], **Franz Bauernfeind**[3,*], **Annett Halle**[1], **Eivind O. Samstad**[1,4], **Hajime Kono**[2], **Kenneth L. Rock**[2], **Katherine A. Fitzgerald**[1], and **Eicke Latz**[1,4,Π]

[1]Department of Infectious Diseases and Immunology, University of Massachusetts Medical School, Worcester, MA 01605, USA

[2]Department of Pathology, University of Massachusetts Medical School, Worcester, MA 01605, USA

[3]Division of Clinical Pharmacology, Department of Internal Medicine, Ludwig-Maximilians-University of Munich, Germany

[4]Institute of Cancer Research and Molecular Medicine, NTNU, N-7489 Trondheim, Norway

Abstract

Inhalation of silica crystals causes inflammation in the alveolar space. Prolonged silica exposure can lead to the development of silicosis, an irreversible, fibrotic pulmonary disease. The mechanisms by which silica and other crystals activate immune cells are not well understood. Here, we demonstrate that silica and aluminum salt crystals activate the NALP3 inflammasome. NALP3 activation requires crystal phagocytosis and crystal uptake leads to lysosomal damage and rupture. Sterile lysosomal damage is also sufficient to induce NALP3 activation and inhibition of phagosomal acidification or cathepsin B impairs NALP3 activation. These results indicate that the NALP3 inflammasome can sense lysosomal damage induced by various means as an endogenous danger signal.

Introduction

Crystalline silica, also known as silicon dioxide (SiO2), is found in nature as sand or quartz. While ingestion of silica is harmless and non-toxic, inhalation of small silica crystals can lead to acute lung inflammation. Chronic, mostly occupational, inhalative silica crystal exposure causes the pneumoconiosis silicosis. Silicosis is an incurable, irreversible, progressive lung fibrosis that is highly associated with other diseases including cardiopulmonary failure, mycobacterial infection, autoimmunity and lung cancer. No effective treatment is currently available for silicosis and the mechanisms of silica crystal-induced lung inflammation and fibrosis are not well understood[1].

Inhalation of silica crystals leads to their deposition in small airways of the lung where mucocilial clearance is not functional. Subsequent ingestion of silica crystals by resident macrophages is known to elicit an inflammatory response that is characterized by the release of cytokines, such as IL-1β and TNFα, and factors that can induce fibrosis. Moreover, silica

Π*Correspondence should be addressed to* Eicke Latz, MD PhD, University of Massachusetts Medical School, 364 Plantation St, LRB 308, Worcester, MA 01605, USA, eicke.latz@umassmed.edu.
*V.H. and F.B. contributed equally to this work.

Author information
The authors declare no competing financial interests.

crystal uptake can initiate apoptotic cell death with concomitant release of ingested silica particles, which are re-engulfed by other alveolar macrophages inducing a cycle of sustained inflammation[2].

Recent reports have revealed that other medically relevant crystals, such as monosodium urate (MSU) or calcium pyrophosphate dihydrate (CPPD) crystals, that trigger inflammation in gout or pseudogout, respectively, can activate the cytoplasmic receptor NACHT-, LRR-, and PYD domain-containing protein 3 (NALP3, also called Cryopyrin/NLRP3)3. NALP3 is a member of a family of cytoplasmic NOD-like receptors (NLRs), which control the activity of the inflammatory caspase-1 by formation of multi-molecular complexes, termed inflammasomes4. Upon activation, NALP3 recruits the adaptor molecule apoptosis-associated speck-like protein (ASC), which, in turn, binds to procaspase-1 leading to its autocatalytic processing and activation5. Active caspase-1 catalyzes the cleavage of the pro-cytokines IL-1β and IL-18 which are only secreted and biologically active in their processed forms6. The upstream mechanisms of NALP3 inflammasome activation are poorly understood. Several ligands of diverse physico-chemical nature have been reported to activate the NALP3 inflammasome. For example, in addition to crystaline MSU and CPPD, bacterial cell wall components, several bacterial toxins and high concentrations of extracellular ATP are all reported to activate the NALP3 inflammasome (reviewed in 4).

Here we investigate the mechanisms of crystal-induced inflammation and demonstrate that, similar to MSU, silica crystals and aluminum salt (alum) crystals activate the NALP3 inflammasome. We further find that NALP3 activation by crystals requires phagocytosis and that phagocytosed crystals induce lysosomal swelling and damage. NALP3 activation by silica crystals is dependent on lysosomal acidification and involves the lysosomal cysteine protease cathepsin B. Crystal-independent lysosomal damage was sufficient to induce NALP3 inflammation. These results suggest a common mechanism of crystal-induced NALP3 inflammasome activation, whereby not the crystal structure itself, but rather lyosomal pertubation is being sensed.

Results

Silica induces release of mature IL-1β and activated caspase-1 in human PBMCs

The NALP3 inflammasome recognizes crystalline material appearing in joint fluids as a danger signal[3]. Inhalation of silica crystals is known to induce a strong pro-inflammatory response including the release of active IL-1β. We thus hypothesized that silica crystals could exert their inflammatory potential via the activation of a similar pathway. Human PBMCs from several donors were incubated with baked LPS-free silica crystals. Pro-IL-1β is not constitutively expressed and requires transcriptional induction in response to e.g. a TLR stimulus. While silica crystals did not induce IL-1β cleavage and release in human PBMCs by themselves, LPS-primed PBMCs strongly responded to the addition of silica crystals in a dose-dependent manner (Fig. 1a). Silica crystal-mediated activation of human PBMCs was as potent as other known activators of the NALP3 inflammasome, such as MSU crystals, ATP or the NALP3-independent stimulus transfected double-stranded DNA (dAdT)[7] (Fig. 1b). IL-1β production as measured by ELISA correlated strongly with the detection of cleaved IL-1β and cleaved caspase-1 as assessed by Western blotting, indicating that activated cells release mature IL-1β. Inhibition of caspase-1 by the specific peptide inhibitor z-YVAD almost completely abolished the IL-1β response in response to silica crystal treatment (Fig. 1c). These data suggest that silica crystals activate IL-1β in a caspase-1 dependent manner in human immune cells.

Silica-mediated neutrophil influx in a model of acute lung inflammation is mediated by IL-1

Exposed individuals inhale silica crystal dust and lung resident immune cells subsequently phagocytose the crystal material and induce an inflammatory response. Large doses of silica dust leads to the clinical syndrome acute silicosis, which is characterized by rapid immune cell influx into the exposed area and massive production of chemokine and proinflammatory cytokines including IL-1β and chemokines[2]. To investigate the *in vivo* relevance of the IL-1 response in silica-induced lung inflammation, wild-type and IL-1 receptor (IL-1R)-deficient mice were transorally instilled with silica crystals and subsequently monitored for acute inflammation after 16–18h. Cells in the bronchoalveolar lavage fluid were counted and their phenotype assessed using flow cytometry analysis. A pronounced lung infiltration of neutrophils was detected in wild-type mice exposed to silica crystals, as compared to those treated with carrier fluid, which was absent in IL-1R-deficient silica crystal exposed mice (Fig. 2a). Other cell types remained largely unchanged (data not shown).

An almost complete abrogation of silica-induced neutrophil influx was also observed in MyD88/TRIF-double-deficient animals, whereas these deletions had little or no effect on zymosan-induced inflammation (Fig. 2b). Commercial zymosan preparations are known to activate TLR2- and Dectin 1-dependent signaling pathways[8, 9], which cooperate to induce cytokines via the adapter molecule MyD88. Together, these results indicate that silica crystals induce IL-1 release and that the IL-1 signal transduction molecules IL-1R and MyD88 play a critical role for the development of acute inflammation *in vivo* following silica crystal exposure.

Silica crystals activate the NALP3 inflammasome

In order to investigate whether silica crystals can activate the NALP3 inflammasome, we performed experiments in murine macrophages from mice deficient in NALP3 or ASC. Similar to their response to known inflammasome activators such as MSU crystals, transfected DNA (dAdT) or ATP, macrophages from wild-type mice produced large amounts of IL-1β upon silica crystal exposure (Fig. 3a, **left panel**). In contrast, macrophages lacking NALP3 or the downstream adapter molecule ASC, failed to release cleaved IL-1β in response to silica crystals (Fig. 3a), indicating the requirement of NALP3 and ASC for IL-1β processing upon silica crystal exposure. Consistent with published reports, MSU crystals and ATP were dependent on both NALP3 and ASC, while transfected dAdT was ASC dependent, yet NALP3 independent (Fig. 3a, **middle and left panel**)[3, 7, 10, 11]. Since IL-1β processing and release could both be influenced by silica crystal activation, we next examined the cleavage of procaspase-1 into active caspase-1. We found that, similar to IL-1β release, caspase-1 cleavage was induced in a dose-dependent manner following silica crystals, MSU, ATP and dAdT (Fig. 3b). This response was completely dependent on ASC for all stimuli since ASC-deficient macrophages failed to trigger caspase-1 cleavage in response to all of these ligands. Consistent with the IL-1β release, caspase-1 cleavage in response to dAdT was independent of NALP3. A recent report implicated uric acid released from cells as a primary trigger for IL-1β production after cell stimulation with other crystal preparations[12]. We tested whether uricase would influence the IL-1b response to MSU or silica crystals and found that the response to silica was unimpaired after incubation with uricase (Fig. 3c). We also generated immortalized macrophage cell lines from wild-type, NALP3- and ASC-deficient mice and examined their response to inflammasome ligands. Immortalized macrophages exhibited qualitatively similar responses as freshly isolated bone-marrow derived macrophages (**see** Supplementary Fig. 1). Collectively, these results clearly suggest that silica crystals activate the NALP3/ASC complex leading to the activation of caspase-1 and subsequent cleavage of pro-IL-1β into mature, secreted IL-1β.

Crystal uptake is required for NALP3 inflammasome activation

In order to decipher the upstream mechanisms involved in silica crystal-induced NALP3 inflammasome activation, we first examined if uptake of crystalline inflammasome activators influenced cell activation. Human PBMCs were pretreated with cytochalasin D, a well-characterized inhibitor of phagocytosis, which impairs actin filament assembly and subsequently stimulated with MSU or silica crystals as well as with two non-crystalline NALP3 activators, ATP and R848[13]. Cytochalasin D completely abrogated IL-1β release following MSU or silica crystals while the response to ATP and R848 was unaffected (Fig. 4a). Similar results were obtained with mouse macrophages (**see** Supplementary Fig. 2a). These results clearly implicate crystal binding and uptake by phagocytosis as prerequisites for activation of the cytosolic NALP3 inflammasome.

In order to visualize the uptake of crystalline material in living cells we devised a method to image crystals simultaneously with cellular components stained with fluorescent dyes (**see** Supplementary Fig. 3). We applied this method to study the uptake of crystals into mouse macrophages. After incubation with silica crystals for 30 min, the cell surface was stained with the membrane binding reagent fluorescent choleratoxin subunit B in the absence or presence of cytochalasin D. Macrophages rapidly phagocytosed crystals into intracellular compartments, while cells that were treated with cytochalasin D failed to phagocytose silca crystals (Fig. 4b) or MSU crystals (**see** Supplementary Fig 2b). The median size of phagocytosed silica crystals was 1.65 μm (Fig 4c).

It is well known that phagocytosis of particulate matter in macrophages results in the generation of reactive oxygen species (ROS). Silica crystals trigger ROS production in macrophages, events reported to be linked to disease pathology in silica-induced inflammation[14]. Based on these reports and our own data highlighting the importance of phagocytosis in silica crystal-induced NALP3 activation, we hypothesized that the phagocyte ROS system might play a role in this response. To address the involvement of this pathway directly, we examined NALP3 inflammasome responses in mice lacking the 91 kDa subunit of the phagosomal NADPH-oxidase cytochrome b (gp91phox). Gp91phox-deficient mice lack phagocyte superoxide production and are reported to be hypersusceptible to various pathogens15. However, macrophages from these mice responded normally to silica crystals, MSU, ATP and dAdT (Fig. 4d). These results indicate that the phagosomal respiratory burst oxidase system is not essential for the activation of the NALP3 inflammasome by these stimuli.

Phagocytosis of crystals leads to lysosomal destabilization

We next performed imaging studies with macrophages undergoing phagocytosis of crystalline material in order to monitor the fate of the phagocytosed cargo. We used confocal reflection microscopy combined with fluorescence imaging to study the subcellular distribution of silica crystals over time. DQ-ovalbumin is a useful tool used to monitor the endo-lysosomal compartment in living cells in real time. The fluorescence of the BODIPY-FL fluorophore on DQ-ovalbumin is normally quenched unless the protein is proteolytically processed into peptides in endo-lysosomal compartments. In untreated cells, processed DQ-ovalbumin was localized to small vesicular and tubular endosomes or lysosomes as expected. In contrast, large swollen lysosomes were detected in the vast majority of cells exposed to silica crystals. In many cells, a cytosolic pattern of fluorescently processed DQ-ovalbumin was observed which indicates lysosomal rupture or leakage of lysosomal contents into the cytosol of crystal treated cells (Fig. 5a). Fluorescent indicator dyes that stain acidic environments corroborated these findings (data not shown). In addition, ingested fluorescent dextran, which traffics into the lysosomal pathway also stained swollen lysosomal compartments and revealed cytosolic translocation in the majority of cells (see

Supplementary Fig. 4). Such swelling of lysosomes was not exclusive to silica crystal treated cells, since MSU crystals evoked similar morphological changes and rupture of lysosomal compartments (data not shown).

We also tested if crystals could be detected in cells outside of phagosomal compartments by staining the plasma membrane and phagosomal membranes with fluorescent choleratoxin b in fixed and permeabilized cells. Most crystals were located in phagosomes that had clear membrane staining, however, some crystals were found in regions, which were not associated with membranes and thus were translocated to the cytosol (Fig 5b). Similar data were obtained when MSU crystals were examined (not shown). In order to quantify the degree of phagosomal rupture upon crystal treatment, we employed acridine orange, a dye used to measure lysosomal integrity. Acridine orange fluoresces green in its monomeric state and binds to nuclear and cytosolic DNA and RNA. Due to its cationic nature, acridine orange becomes highly concentrated in acidic compartments resulting in dimerization and appearance of red fluorescence (**see** Supplementary Fig. 5). The amount of red lysosome fluorescence of acridine orange directly correlates to the amount of acidic lysosomes in cells. We took advantage of this property and monitored lysosome content in macrophages before and after treatment with silica crystals. Increasing amounts of silica crystals resulted in loss of lysosomes as indicated by reduced red acridine orange fluorescence (Fig. 5c, **upper panel**). Furthermore, lysosomal rupture due to silica phagocytosis was observed to a similar extent in cells deficient in NALP3, which indicates that lysosomal damage is independent of NALP3 (Fig. 5c, **lower panel**). Collectively, these data demonstrate that phagocytosis of crystalline material leads to active swelling of phagosomes followed by phagosomal destabilization and rupture, thus releasing phagosomal contents which then gain access to the cytosolic compartment.

Lysosomes contain a plethora of proteolytic enzymes, many of which are activated by acidification of lysosomal pathways. To assess the role of lysosomal acidification in silica-mediated NALP3 activation, we used bafilomycin A to block the vacuolar H+ATPase system, which is required for acidification of lysosomal compartments. As expected, bafilomycin A blocked formation of acidic lysosomes in macrophages, which was assessed using a lysomotropic pH sensitive dye (lysosensor green), which only fluoresces upon accumulation in acidic environments (Fig. 5d). In addition, bafilomycin A suppressed the rapid, dose dependent appearance of fluorescent DQ-ovalbumin (Fig. 5e) indicating a reduction of lysosomal proteolytic function. Notably, bafilomyin A completely blocked silica-mediated IL-1β release, but had no effect on ATP (Fig. 5f) suggesting a pivotal role of lysosomal function for crystal-mediated NALP3 activation.

Crystal-induced lysosomal destabilization triggers inflammasome activation

Since one important function of lysosomal acidification is the pH-dependent activation of proenzymes to further degrade lysosomal contents, we hypothesized that activation of lysosomal proenzymes could constitute a critical event in silica-mediated inflammasome activation. In particular the cathepsin family of proenzymes were likely candidates. To address their role in silica-mediated inflammasome activation, we tested several cathepsin inhibitors for their ability to affect silica-mediated IL-1β release. Among the inhibitors tested, CA-074-Me, a cathepsin B-specific inhibitor[16], led to a markedly reduced caspase-1 activation upon silica crystal treatment (Fig. 6a). Matured cathepsin B could also be detected in supernatants of crystal stimulated cells, independent of NALP3 (Fig. 6b). In order to assess whether cathepsin B release from lysosomes was timely associated with caspase-1 activation, we incubated mouse macrophages with silica crystals and added fluorescent peptides that indicate cathepsin B activity by and increase of red fluorescence and caspase-1 activity by green fluorescence. When resting cells were incubated with these two reporter peptides, red fluorescence was observed in lysosomal compartments indicative of cathepsin

B activity, while resting cells did not acquire green fluorescence due to lack of caspase-1 activity (Fig. 6c, **left panel**). Cells that were treated with silica crystals, acquired either red fluorescence due to lysosomal containment of the cathepsin B indicator peptide or green cytoplasmic fluorescence indicative of caspase-1 activity (Fig. 6c, **right panel**). Activated cells obtained from caspase-1 deficient macrophages did not stain with the caspase-1 fluorescent peptide demonstrating specificity of the reagent (data not shown). This striking difference between staining of either lysosomal cathepsin B or activated caspase-1 suggests that cells which lose lysosomal cathepsin B upon lysosomal rupture (loss of red lysosomal fluorescence) rapidly activate caspase-1. Together, these results suggest that the NALP3 inflammasome senses lysosomal contents released into the cytosol of phagocytic macrophages after crystal-induced lysosomal damage.

Aluminium salts (alum) are the most commonly used vaccine adjuvants and all alum preparations contain crystals. Recently, aluminium hydroxide was reported to induce the cleavage of IL-1β and IL-18 in a caspase-1-dependent manner[17]. To determine whether alum induces inflammation via a mechanism similar to silica crystals, we performed experiments with a mixture of aluminum hydroxide and magnesium hydroxide (imject alum). Alum induced IL-1β maturation and release in human PBMCs (Fig. 7a) in a caspase-1-dependent manner (not shown). In murine macrophages, alum-induced IL-1β release was dependent on NALP3 and ASC (Fig. 7b) indicating that alum triggers inflammation via NALP3 inflammasome activation. Additionally, peritoneal neutrophil influx after intraperitoneal alum administration was highly dependent on IL-1 activity (Fig. 7c). Of note, alum added to cells induced marked morphological changes and led to lysosomal rupture, as evidenced cytosolic DQ ovalbumin translocation (Fig. 7d) and acridine orange lysosomal staining pattern (Fig. 7e). As observed with silica crystals, cells incubated with alum stained either positively with a cathepsin B indicator or the caspase-1 indicator (Fig. 7f), which demonstrates a close correlation of lysosomal loss and caspase-1 activation. In agreement with this notion, alum-induced IL-1β release was found to be partially dependent on lysosomal acidification and cathepsin B activity (Fig. 7g). Uriase added to crystal- or ATP-stimulated cells dose-dependently inhibited MSU crystal elicited IL-1β release but did not change the response to alum (Fig. 7h).

Crystal independent lysosomal damage activates the NALP3 inflammasome

To determine if lysosomal rupture alone were sufficient to activate the inflammasome, we turned to a model in which we could assess the role of lysosomal rupture without the requirement of the addition of known inflammasome activators. Mouse macrophages were loaded with a hypertonic solution and subsequently placed in hypotonic media resulting in rupture of endo-lysosomal compartments. As shown in Fig 8a, employing this strategy successfully translocated endo-lysosomal fluorescent dextran into the cytosol, as evidenced by a diffuse cytosolic staining of cells after the treatment. Following this crystal-independent disruption of lysosomes, caspase-1 cleavage could be observed (Fig. 8b, **left**) which was partially inhibited by a cathepsin B inhibitor. Importantly, this crystal-independent lysosomal rupture was completely dependent on NALP3 (Fig. 8b, **right**). Together, these results indicate that rupture of lysosomal compartments and leakage of lysosomal contents into the cytosol even in the absence of crystal material was sufficient to trigger NALP3 inflammasome activation in a partially cathepsin B-dependent manner.

Additionally, we used THP-1 cells differentiated in the presence of PMA in this lysosomal rupture assay, representing a model system that does not rely on microbial stimuli for pro-IL-1β priming. Similar to the findings with mouse macrophages, THP-1 cells were also activated to release cleaved IL-1β after lysosomal rupture in a partially cathepsin B-dependent manner (**see** Supplementary Fig. 6).

In order to corroborate these findings, we employed an alternative method to disrupt lysosomes and used the lysomotropic reagent L-leucyl-L-leucine methyl ester (Leu-Leu-OMe) that is known to induce lysosomal damage [18, 19]. Leu-Leu-OMe is a functionalized dipeptide, which is converted to a membranolytic compound by the lysosomal enzyme dipeptidyl peptidase I. We incubated mouse macrophages with Leu-Leu-OMe at reported effective doses and observed a pronounced swelling and rupture of lysosomes in the majority of cells as indicated by lysosomal morphology, loss of red acridine orange fluorescence and diffuse cytoplasmic staining of fluorescent dextran (Fig. 8c). Inhibition of lysosomal acidification by bafilomycin markedly reduced the altered lysosomal morphology and rupture (not shown). We next assessed whether Leu-Leu-OMe activated Il-1β maturation. We detected large quantities of IL-1β in cellular supernatants in response to Leu-Leu-OMe, similar to concentrations that were elicited by known inflammasome activators (Fig. 8d). To test whether the Leu-Leu-OMe-induced lysosomal damage induces NALP3 activation, we analyzed macrophages from mice deficient in NALP3 and ASC. As observed with silica crystals, NALP3 and ASC knock-out cells failed to respond to Leu-Leu-OMe-induced lysosomal damage and did only release minor quantities of IL-1β (Fig. 8e). Finally, inhibition of lysosomal pH by bafilomycin or inhibition of cathepsin B also inhibited the release of IL-1β in response to Leu-Leu-OMe (Fig. 8e).

Discussion

Chemically and structurally diverse stimuli, ranging from the small molecules ATP or imidazoquinoline derivatives (R848, R837), to bacterial toxins and various crystals, can activate the NALP3 inflammasome[4]. Undoubtedly, the list of NALP3 inflammasome activators will grow, yet the mechanisms by which the NALP3 inflammasome can sense different activators are not yet fully understood. One possibility is that NALP3 acts as a pattern recognition receptor that can directly bind and respond to various ligands. Indeed, recent reports suggest that NALP3 activators could gain access to the cytoplasmic space[20, 21]. A precedent for such a mechanism is given by the large spectrum of ligands that can be sensed by certain Toll like receptors[22].

Another possibility is that the NALP3 inflammasome detects an intermediate molecule that is generated by a common mechanism evoked by many different ligands. It has been shown that potassium efflux is required for NALP3 activation upon various inflammasome stimuli[23, 24]. However, it is currently unclear whether potassium efflux alone represents a NALP3 inflammasome stimulus *per se* or whether low intracellular potassium acts as an additional requirement for inflammasome assembly after appearance of an as of yet undefined primary stimulus. An example of this potential mechanism is found in the formation of the closely related apoptosome[25, 26]. The loss of intracellular potassium during apoptosis is an early, essential step for successful assembly of the apoptosome, which forms after cytochrome c is released from mitochondria in stress situations. It is therefore possible, that formation of the NALP3 inflammasome is highly favored at low intracellular potassium levels, which may be required yet not sufficient for activation.

We show here the novel finding that NALP3 inflammasome activation by crystals or alternatively induced lysosomal damage requires uptake and acidification of lysosomes and that the ingested crystals lead to lysosomal swelling and leakage. Notably, inhibition of a single lysosomal protease - cathepsin B – led to substantial, yet not complete, reduction of NALP3 inflammasome activation by lysosomal damage. In this context it is noteworthy that the NALP3 stimulus nigericin, which is thought to solely activate via potassium efflux, has induced lysosomal leakage and subsequent caspase-1 activation via the function of cathepsin B[27]. Since it was also shown that pannexin 1, which helps establishing larger lysosomal channels, was required for nigericin-mediated NALP3 activation[28, 29], it is conceivable that

pannexin 1 does not only allow access of bacterial ligands to the cytoplasm[20, 21] but could also initiate lysosomal destabilization. Others have also suggested a role for cathepsin B in NALP3 inflammasome function, yet their data implied a role for cathepsin B downstream[30, 31] rather than upstream of NALP3, as we have demonstrated here. It will be important to define molecular targets of cathepsin B and potentially other pH-activated proteases, as this may guide us to common upstream NALP3 activating factors. It was recently shown that a related cathepsin (cathepsin K) is also involved in innate immune recognition. Cathepsin K acts upstream of the innate signaling receptor TLR9[32], which signals from within endo-lysosomal compartments[33, 34].

Collectively, our data suggest the hypothesis that lysosomal damage or leakage is perceived by the immune system as an endogenous danger signal. The NALP3 inflammasome can respond to internal membrane perturbations and thereby respond to different stimuli, which all have in common that they can induce lysosomal destabilization. Phagocytes that ingest endogenous or exogenous crystallized material or potentially also aggregated proteins or peptides are thus capable of sensing lysosomal damage induced by the phagocytosed cargo. Following NALP3 inflammasome activation highly inflammatory cytokines are generated, which leads to the recruitment of other immune cells to the affected tissue and to the induction of inflammatory mechanisms that assist in the clearance of the crystallized material. However, it is also possible that NALP3 activation by this mechanism can lead to sustained inflammation and resulting tissue damage. For example, chronic inhalative exposure to silica or asbestos can lead to chronic inflammation, tissue damage and carcinogenesis.

NALP3 activation by particulate matter can also intentionally be exploited therapeutically. Aluminium salt preparations, which are commonly used as adjuvants, contain small crystalline materials. We demonstrated here that alum activates immune cells via the NALP3 inflammasome, by a mechanism that involves lysosomal destabilization. It is likely that other vaccine candidates that are of particulate nature or that can perturb lysosomal membranes act via a similar NALP3 activation mechanism.

Our findings should thus aid in the development of novel vaccines and can lead to novel therapeutic concepts for the treatment of NALP3 inflammasome related pathologies.

Methods

Mice

NALP3[13]-, ASC[13]- and IPAF[36]-deficient mice were kindly provided by Millennium Pharmaceuticals (Cambridge, MA). C57BL/6 mice, 129/Sv mice, C57/Bl6 × 129 F1 mice, IL-1R$^{-/-}$ and gp91phox$^{-/-}$ were purchased from Jackson Laboratories (Bar Harbor, ME). MyD88$^{-/-}$-TRIF$^{-/-}$ mice were generated from MyD88$^{-/-}$ and TRIF$^{-/-}$ mice, kindly provided by Shizuo Akira (Kyoto, Japan). Seven to nine week-old animals were used in all experiments. All mouse strains were bred and maintained under specific pathogen-free conditions in the animal facilities at the University of Massachusetts Medical School. All experiments involving live animals were carried out in accordance with the guidelines set forth by the University of Massachusetts Medical School Department of Animal Medicine and the Institutional Animal Care and Use Committee.

Reagents

Acridine orange, ATP, bafilomycin A1, cytochalasin D, LPS, PMA, poly(deoxyadenylic-thymidylic) acid sodium salt (dAdT), sucrose and zymosan were purchased from Sigma-Aldrich (St. Louis, MO). CA-074-Me and PEG 1000 were purchased from Calbiochem (Gibbstown, NJ). DQ-ovalbumin, A647-conjugated dextran, A647-conjugated choleratoxin

B, lysosensor green and Hoechst stain were obtained from Molecular Probes, Invitrogen (Carlsbad, CA). Alum (Imject Alum Adjuvant, mixture of aluminum hydroxide and magnesium hydroxide) was purchased from Pierce (Rockford, IL). Leu-Leu-OMe·HCl was purchased from Chem-Impex International (Wood Dale, IL). Uricase (Elitek™) was purchased from Sanofi-Aventis (Bridgewater, NJ).

Silica crystals (MIN-U-SIL-15) were kindly provided by U.S. Silica Company (Berkeley Springs, WV). Throughout the study, a polydispersed preparation of silica crystals of up to 15 μm were used. MSU crystals were prepared as previously described[37].

In vivo silica model

Mice were exposed to 40 μl aqueous suspensions of 200 μg of silica crystals (MIN-U-SIL-15) in PBS or 50 μg crude zymosan by direct orotracheal instillation. Control mice received PBS. Animals were sacrificed 16–18 hours after instillation and a bronchoalveolar lavage (BAL) was carried out by repeatedly instillating and withdrawing 1 ml of 1% BSA / PBS solution three consecutive times. Recovered BAL fluid was pelleted by centrifugation and counted. Subsequently, cells were stained for surface markers and neutrophils were identified as double positive cells for MCA771B (Serotec, Raleigh NC) and Ly6G (BD Biosciences) using flow cytometry. For alum experiments, mice were injected i.p. with 100 μg of a mixture of aluminum hydroxide and magnesium hydroxide (Pierce, Rockford, IL) in 200μl PBS. 16–18h after challenge, animals were euthanized and their peritoneal cavities were washed with 6 ml PBS containing 3 mM EDTA and 10 U/ml heparin. Total numbers of peritoneal exudate cells were counted by a hematocytometer, and the numbers of neutrophils were evaluated as described above.

Cell isolation and culture

Bone marrow derived macrophages were generated as described[38]. Human PBMCs were isolated by from whole blood of healthy volunteers by density gradient centrifugation. Lysis of red blood cells was performed using red blood cell lysis buffer (Sigma). Experiments in PBMCs and macrophages were carried out at a cell density of 2×10^6 cells / ml. All primary cells and cell lines except THP-1 cells were cultured in DMEM supplemented with L-glutamine, ciprofloxacin (Cellgro, Manassas, VA) and 10% fetal calf serum (Hyclone, Logan, UT). THP-1 cells were cultured in RPMI supplemented with 10% fetal calf serum (Hyclone), L-glutamine, sodium pyruvate (Cellgro), and ciprofloxacin. One day prior to stimulation, THP-1 cells were differentiated using 0.5 μM PMA for three hours, washed three times and plated for stimulation. All experiments that were performed for Western blot analysis were carried out in serum free DMEM medium. ATP stimulations were carried out at 5 mM one hour prior to harvesting supernatants.

Immortalized macrophage cell lines

Immortalized macrophage cell lines were generated using the previously described J2 recombinant retrovirus (carrying v-myc and v-raf/mil oncogenes)[39]. Briefly, primary bone marrow cells were incubated in L929 conditioned medium for 3–4 days to induce macrophage differentiation. Subsequently, cells were infected with J2 recombinant retrovirus. Cells were maintained in culture for 3–6 months slowly weaning off the percentage of L929 supernatant until cells were growing in the absensce of conditioned medium. Macrophage phenotype was verified by surface marker expression for CD11b and F480 as well as a range of functional parameters, including responsiveness to TLR ligands and bacterial uptake. Macrophage cell lines from wild-type (C57BL6), NALP3- and ASC-deficient mice were generated and are referred to as B6-MCLs, NALP3-MCLs and ASC-MCLs.

Flow cytometry analysis

For evaluation of lysosomal rupture, cells were incubated with 1 μg/ml acridine orange for 15 min, washed three times and subsequently stimulated as indicated. Lysosomal rupture can be assessed by loss of emission at 600–650 nm using flow cytometry. All flow cytometry experiments were performed on an LSRII cytometer (BD Biosciences). Data were acquired by DIVA (BD Biosciences) and analyzed by FlowJo software (Tree Star Inc., Ashland, OR).

Confocal microscopy

Confocal reflection microscopy was combined with fluorescence microscopy on a Leica SP2 AOBS confocal laser scanning microscope. Reflection was captured by placing the detector channel directly over the wavelength of the selected laser channel for reflection light capture and the AOBS was set to allow 5–15% of laser light into the collection channel. Fluorescence was simultaneously captured by standard confocal imaging techniques.

ELISA

Cell culture supernatants were assayed for IL-1β using ELISA kits from BD Biosciences (Franklin Lakes, NJ) according to the manufacturer's instructions. To measure intracellular IL-1β, cells were washed and subjected to three freeze thaw cycles in assay diluent.

Lysosomal rupturing in THP-1 cells

PMA-differentiated THP-1 cells were incubated with hypertonic DMEM medium containing 10% polyethylene glycol (PEG) 1000, 1.4 M sucrose, 20 mM Hepes (pH 7.2) and 5% FCS for 10 min at 37°C. Cells were subsequently washed and incubated in hypotonic DMEM medium [DMEM : H_2O (3:2)] for 2 min to induce lysosomal rupturing. Cells were then incubated in serum free DMEM for additional 4 hours.

Staining of cathepsin B and caspase-1

After treatement as indicated, cells were incubated with the fluorescent cathepsin B substrate Magic Red (cresyl violet, bisubstituted via amide linkage to the dipeptide arginine-arginine) together with the FLICA caspase-1 green fluorescent peptide (FAM-YVAD-FMK) for 30 min at 37 C per the recommendations of the manufacturer (Immunochemistry Technologies, Bloomington, MN). After three washes in PBS, cells were visualized by confocal microscopy.

Western blot analysis

Cell culture supernatants were precipitated by adding an equal volume of methanol and 0.25 volumes of chloroform, vortexed and centrifuged at 20.000 × g for 10 min. The upper phase was discarded and 500 μl of methanol was added to the interphase. This mixture was centrifuged at 20.000 × g for 10 min and the protein pellet dried at 55 °C, resuspended in Laemmli buffer and boiled at 99°C for 5 min. Samples were separated by SDS-PAGE (15%) and transferred onto nitrocellulose membranes. As indicated, blots were incubated with rabbit polyclonal antibody to anti murine caspase-1 p10 (sc-514, Santa Cruz Biotechnology, Santa Cruz, CA), rabbit polyclonal anti human caspase-1 p10 (sc-515, Santa Cruz Biotechnology), rabbit polyclonal anti human cleaved IL-1β (Asp116) (Cell Signaling, Boston, MA) or rabbit polyclonal anti murine cathepsin B (R&D Systems, Minneapolis, MN).

Supplementary Material

Refer to Web version on PubMed Central for supplementary material.

Acknowledgments

The authors would like to acknowledge Anna Cerny and Joseph Boulanger for animal husbandry and genotyping and Douglas Golenbock for providing J2 recombinant retroviruses. V.H. is supported by the DFG Ho2783/2–1. E.L. and K.A.F. are supported by grants from the NIH. Jinhee Lee and Hardy Kornfeld are thanked for help with the lung inflammation model.

References

1. Mossman BT, Churg A. Mechanisms in the pathogenesis of asbestosis and silicosis. American journal of respiratory and critical care medicine 1998;157:1666–1680. [PubMed: 9603153]
2. Huaux F. New developments in the understanding of immunology in silicosis. Current opinion in allergy and clinical immunology 2007;7:168–173. [PubMed: 17351471]
3. Martinon F, Petrilli V, Mayor A, Tardivel A, Tschopp J. Gout-associated uric acid crystals activate the NALP3 inflammasome. Nature 2006;440:237–241. [PubMed: 16407889]
4. Petrilli V, Dostert C, Muruve DA, Tschopp J. The inflammasome: a danger sensing complex triggering innate immunity. Current opinion in immunology 2007;19:615–622. [PubMed: 17977705]
5. Agostini L, Martinon F, Burns K, McDermott MF, Hawkins PN, Tschopp J. NALP3 forms an IL-1beta-processing inflammasome with increased activity in Muckle-Wells autoinflammatory disorder. Immunity 2004;20:319–325. [PubMed: 15030775]
6. Dinarello CA. Interleukin-1 beta, interleukin-18, and the interleukin-1 beta converting enzyme. Annals of the New York Academy of Sciences 1998;856:1–11. [PubMed: 9917859]
7. Muruve DA, Petrilli V, Zaiss AK, White LR, Clark SA, Ross PJ, Parks RJ, Tschopp J. The inflammasome recognizes cytosolic microbial and host DNA and triggers an innate immune response. Nature 2008;452:103–107. [PubMed: 18288107]
8. Ozinsky A, Underhill DM, Fontenot JD, Hajjar AM, Smith KD, Wilson CB, Schroeder L, Aderem A. The repertoire for pattern recognition of pathogens by the innate immune system is defined by cooperation between toll-like receptors. Proceedings of the National Academy of Sciences of the United States of America 2000;97:13766–13771. [PubMed: 11095740]
9. Brown GD, Taylor PR, Reid DM, Willment JA, Williams DL, Martinez-Pomares L, Wong SY, Gordon S. Dectin-1 is a major beta-glucan receptor on macrophages. The Journal of experimental medicine 2002;196:407–412. [PubMed: 12163569]
10. Mariathasan S, Weiss DS, Newton K, McBride J, O'Rourke K, Roose-Girma M, Lee WP, Weinrauch Y, Monack DM, Dixit VM. Cryopyrin activates the inflammasome in response to toxins and ATP. Nature 2006;440:228–232. [PubMed: 16407890]
11. Mariathasan S, Newton K, Monack DM, Vucic D, French DM, Lee WP, Roose-Girma M, Erickson S, Dixit VM. Differential activation of the inflammasome by caspase-1 adaptors ASC and Ipaf. Nature 2004;430:213–218. [PubMed: 15190255]
12. Kool M, Soullie T, van Nimwegen M, Willart MA, Muskens F, Jung S, Hoogsteden HC, Hammad H, Lambrecht BN. Alum adjuvant boosts adaptive immunity by inducing uric acid and activating inflammatory dendritic cells. The Journal of experimental medicine 2008;205:869–882. [PubMed: 18362170]
13. Kanneganti TD, Ozoren N, Body-Malapel M, Amer A, Park JH, Franchi L, Whitfield J, Barchet W, Colonna M, Vandenabeele P, Bertin J, Coyle A, Grant EP, Akira S, Nunez G. Bacterial RNA and small antiviral compounds activate caspase-1 through cryopyrin/Nalp3. Nature 2006;440:233–236. [PubMed: 16407888]
14. Fubini B, Hubbard A. Reactive oxygen species (ROS) and reactive nitrogen species (RNS) generation by silica in inflammation and fibrosis. Free radical biology & medicine 2003;34:1507–1516. [PubMed: 12788471]
15. Pollock JD, Williams DA, Gifford MA, Li LL, Du X, Fisherman J, Orkin SH, Doerschuk CM, Dinauer MC. Mouse model of X-linked chronic granulomatous disease, an inherited defect in phagocyte superoxide production. Nature genetics 1995;9:202–209. [PubMed: 7719350]
16. Buttle DJ, Murata M, Knight CG, Barrett AJ. CA074 methyl ester: a proinhibitor for intracellular cathepsin B. Archives of biochemistry and biophysics 1992;299:377–380. [PubMed: 1444478]

17. Li H, Nookala S, Re F. Aluminum hydroxide adjuvants activate caspase-1 and induce IL-1beta and IL-18 release. J Immunol 2007;178:5271–5276. [PubMed: 17404311]
18. Thiele DL, Lipsky PE. Regulation of cellular function by products of lysosomal enzyme activity: elimination of human natural killer cells by a dipeptide methyl ester generated from L-leucine methyl ester by monocytes or polymorphonuclear leukocytes. Proceedings of the National Academy of Sciences of the United States of America 1985;82:2468–2472. [PubMed: 3857595]
19. Thiele DL, Lipsky PE. Mechanism of L-leucyl-L-leucine methyl ester-mediated killing of cytotoxic lymphocytes: dependence on a lysosomal thiol protease, dipeptidyl peptidase I, that is enriched in these cells. Proceedings of the National Academy of Sciences of the United States of America 1990;87:83–87. [PubMed: 2296607]
20. Kanneganti TD, Lamkanfi M, Kim YG, Chen G, Park JH, Franchi L, Vandenabeele P, Nunez G. Pannexin-1-mediated recognition of bacterial molecules activates the cryopyrin inflammasome independent of Toll-like receptor signaling. Immunity 2007;26:433–443. [PubMed: 17433728]
21. Marina-Garcia N, Franchi L, Kim YG, Miller D, McDonald C, Boons GJ, Nunez G. Pannexin-1-Mediated Intracellular Delivery of Muramyl Dipeptide Induces Caspase-1 Activation via Cryopyrin/NLRP3 Independently of Nod2. J Immunol 2008;180:4050–4057. [PubMed: 18322214]
22. Takeda K, Kaisho T, Akira S. Toll-like receptors. Annual review of immunology 2003;21:335–376.
23. Petrilli V, Papin S, Dostert C, Mayor A, Martinon F, Tschopp J. Activation of the NALP3 inflammasome is triggered by low intracellular potassium concentration. Cell death and differentiation 2007;14:1583–1589. [PubMed: 17599094]
24. Franchi L, Kanneganti TD, Dubyak GR, Nunez G. Differential requirement of P2×7 receptor and intracellular K+ for caspase-1 activation induced by intracellular and extracellular bacteria. The Journal of biological chemistry 2007;282:18810–18818. [PubMed: 17491021]
25. Cain K, Bratton SB, Cohen GM. The Apaf-1 apoptosome: a large caspase-activating complex. Biochimie 2002;84:203–214. [PubMed: 12022951]
26. Karki P, Seong C, Kim JE, Hur K, Shin SY, Lee JS, Cho B, Park IS. Intracellular K(+) inhibits apoptosis by suppressing the Apaf-1 apoptosome formation and subsequent downstream pathways but not cytochrome c release. Cell death and differentiation 2007;14:2068–2075. [PubMed: 17885667]
27. Hentze H, Lin XY, Choi MS, Porter AG. Critical role for cathepsin B in mediating caspase-1-dependent interleukin-18 maturation and caspase-1-independent necrosis triggered by the microbial toxin nigericin. Cell death and differentiation 2003;10:956–968. [PubMed: 12934070]
28. Pelegrin P, Surprenant A. Pannexin-1 mediates large pore formation and interleukin-1beta release by the ATP-gated P2×7 receptor. The EMBO journal 2006;25:5071–5082. [PubMed: 17036048]
29. Pelegrin P, Surprenant A. Pannexin-1 couples to maitotoxin- and nigericin-induced interleukin-1beta release through a dye uptake-independent pathway. The Journal of biological chemistry 2007;282:2386–2394. [PubMed: 17121814]
30. Fujisawa A, Kambe N, Saito M, Nishikomori R, Tanizaki H, Kanazawa N, Adachi S, Heike T, Sagara J, Suda T, Nakahata T, Miyachi Y. Disease-associated mutations in CIAS1 induce cathepsin B-dependent rapid cell death of human THP-1 monocytic cells. Blood 2007;109:2903–2911. [PubMed: 17164343]
31. Willingham SB, Bergstralh DT, O'Connor W, Morrison AC, Taxman DJ, Duncan JA, Barnoy S, Venkatesan MM, Flavell RA, Deshmukh M, Hoffman HM, Ting JP. Microbial pathogen-induced necrotic cell death mediated by the inflammasome components CIAS1/cryopyrin/NLRP3 and ASC. Cell host & microbe 2007;2:147–159. [PubMed: 18005730]
32. Asagiri M, Hirai T, Kunigami T, Kamano S, Gober HJ, Okamoto K, Nishikawa K, Latz E, Golenbock DT, Aoki K, Ohya K, Imai Y, Morishita Y, Miyazono K, Kato S, Saftig P, Takayanagi H. Cathepsin K-dependent toll-like receptor 9 signaling revealed in experimental arthritis. Science (New York, N.Y 2008;319:624–627.
33. Latz E, Schoenemeyer A, Visintin A, Fitzgerald KA, Monks BG, Knetter CF, Lien E, Nilsen NJ, Espevik T, Golenbock DT. TLR9 signals after translocating from the ER to CpG DNA in the lysosome. Nature immunology 2004;5:190–198. [PubMed: 14716310]

34. Latz E, Verma A, Visintin A, Gong M, Sirois CM, Klein DC, Monks BG, McKnight CJ, Lamphier MS, Duprex WP, Espevik T, Golenbock DT. Ligand-induced conformational changes allosterically activate Toll-like receptor 9. Nature immunology 2007;8:772–779. [PubMed: 17572678]

35. Dostert C, Petrilli V, Van Bruggen R, Steele C, Mossman BT, Tschopp J. Innate Immune Activation Through Nalp3 Inflammasome Sensing of Asbestos and Silica. Science (New York, N.Y. 2008

36. Franchi L, Amer A, Body-Malapel M, Kanneganti TD, Ozoren N, Jagirdar R, Inohara N, Vandenabeele P, Bertin J, Coyle A, Grant EP, Nunez G. Cytosolic flagellin requires Ipaf for activation of caspase-1 and interleukin 1beta in salmonella-infected macrophages. Nature immunology 2006;7:576–582. [PubMed: 16648852]

37. Schiltz C, Liote F, Prudhommeaux F, Meunier A, Champy R, Callebert J, Bardin T. Monosodium urate monohydrate crystal-induced inflammation in vivo: quantitative histomorphometric analysis of cellular events. Arthritis and rheumatism 2002;46:1643–1650. [PubMed: 12115197]

38. Severa M, Coccia EM, Fitzgerald KA. Toll-like receptor-dependent and -independent viperin gene expression and counter-regulation by PRDI-binding factor-1/BLIMP1. The Journal of biological chemistry 2006;281:26188–26195. [PubMed: 16849320]

39. Roberson SM, Walker WS. Immortalization of cloned mouse splenic macrophages with a retrovirus containing the v-raf/mil and v-myc oncogenes. Cellular immunology 1988;116:341–351. [PubMed: 2460250]

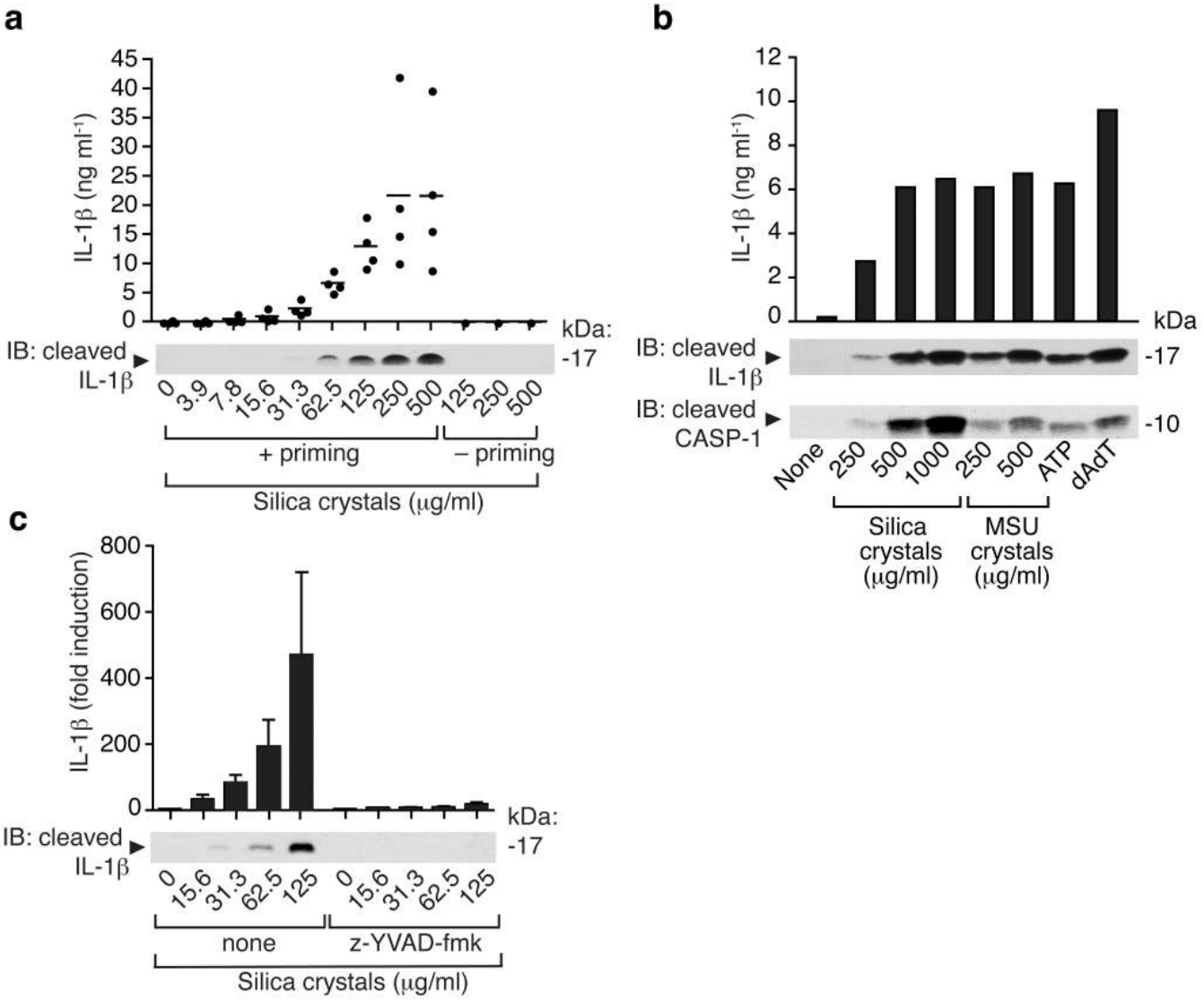

Fig. 1. Silica induces release of mature IL-1β and activated caspase-1 in human PBMCs in a caspase-1 dependent manner

(a) Human PBMCs were primed with LPS (25 pg/ml) or left untreated for 3h and subsequently stimulated with silica crystals or controls. After 6h, supernatants were assessed for IL-1β production by ELISA and Western blot. ELISA data of four independent donors are depicted (upper panel) and Western blot analysis of one representative donor is shown (lower panel). **(b)** LPS-primed human PBMCs were stimulated with either silica crystals, MSU crystals, ATP or transfected with dAdT. 6h after stimulation, supernatants were analyzed for IL-1β by ELISA and assessed for matured IL-1β or activated caspase-1 by Western blot. Data of one representative donor out of three are depicted. **(c)** Human LPS-primed PBMCs were stimulated with silica crystals in the presence or absence of the caspase-1 inhibitor z-YVAD (10 μM). After 6h, supernatants were assessed for IL-1β by ELISA and Western blot. Mean values (+SD) of two donors are depicted as fold increase (ELISA) and Western blot data of one representative donor are shown.

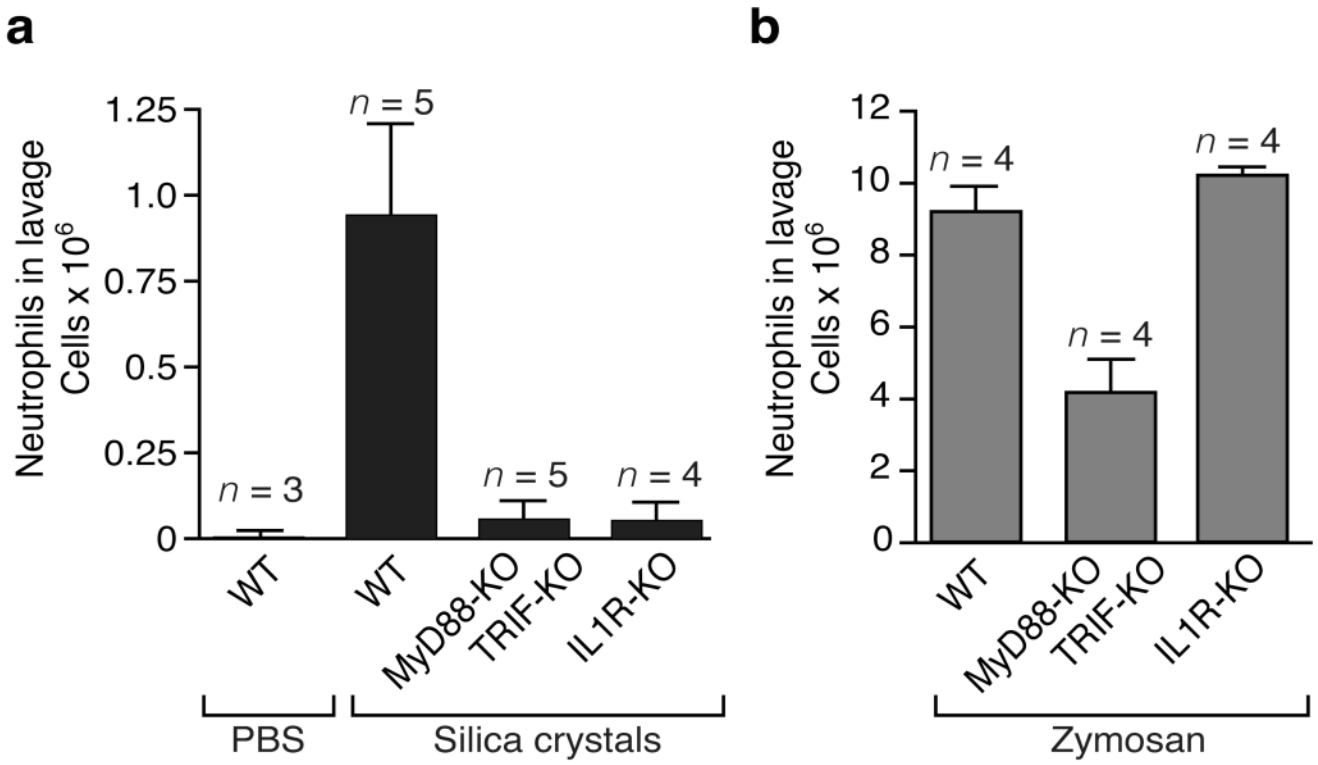

Fig. 2. Silica-mediated neutrophil influx in a model of acute lung inflammation is mediated by IL-1

(a) Silica crystals (200 μg / mouse) were orotracheally instilled into wild-type mice, MyD88/TRIF-double-deficient mice or IL-1R-deficient mice. 16–18h after instillation, neutrophil counts were monitored in the lung lavage by FACS. **(b)** In addition, wild-type mice, MyD88-/TRIF-double-deficient mice or IL-1R-deficient mice were orotracheally challenged with zymosan (50 μg / mouse) and processed as in (a).

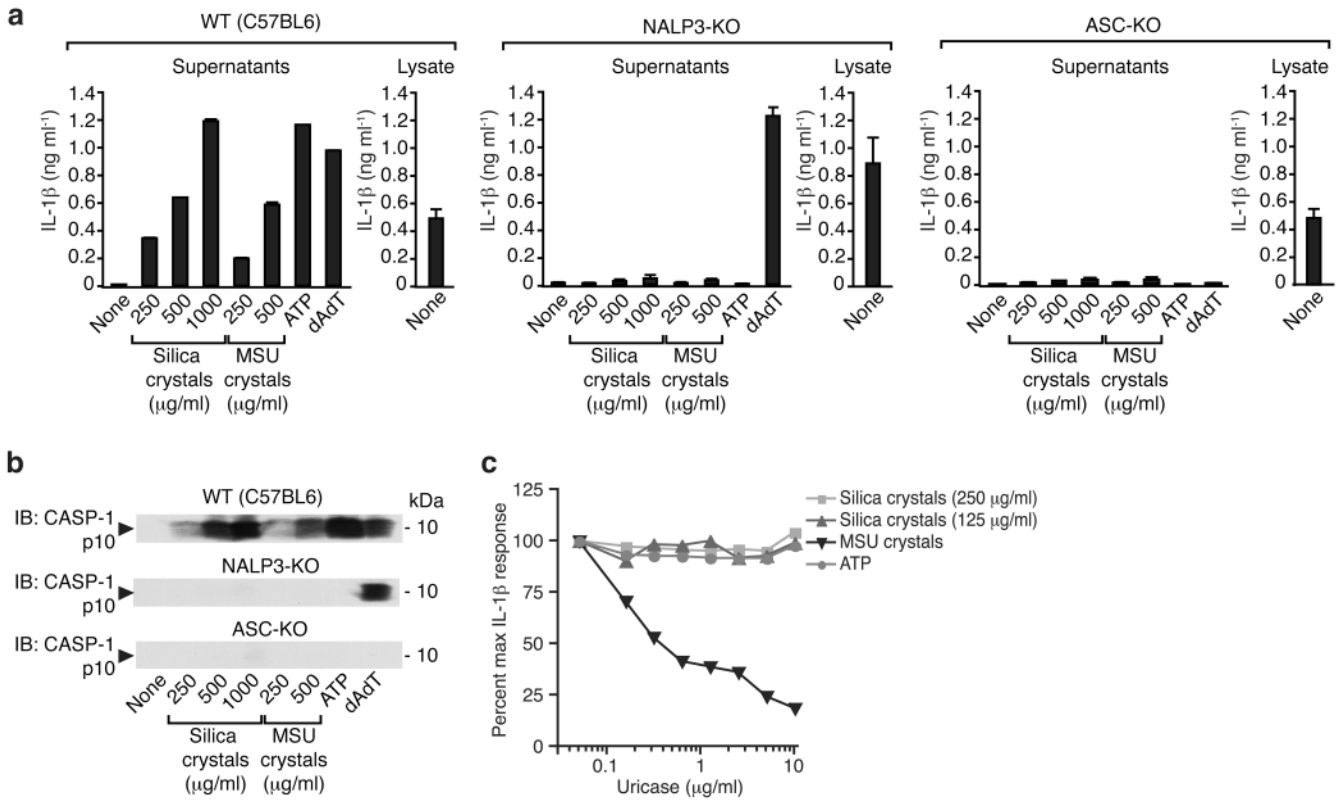

Fig. 3. Silica-mediated release of matured IL-1β and activated caspase-1 is mediated by the NALP3 inflammasome

(a) Bone marrow-derived macrophages of wild-type mice, NALP3-deficient mice or ASC-deficient mice were primed with LPS for 3h and subsequently stimulated with either silica crystals, MSU crystals, ATP or transfected with dAdT. 6h after stimulation, supernatants were analyzed for IL-1β by ELISA (supernatants). To assess intracellular pro-IL-1β, cell lysates from primed, but unstimulated macrophages were assessed for IL-1β by ELISA (lysate). **(b)** In addition, supernatants were assessed for activated caspase-1 by Western blot. Data from one representative experiment out of two are depicted. **(c) LPS-primed mouse macrophages were stimulated with silica or MSU crystals as indicated in absence or presence of uricase as shown. Supernatants were assessed for IL-1β by ELISA**.

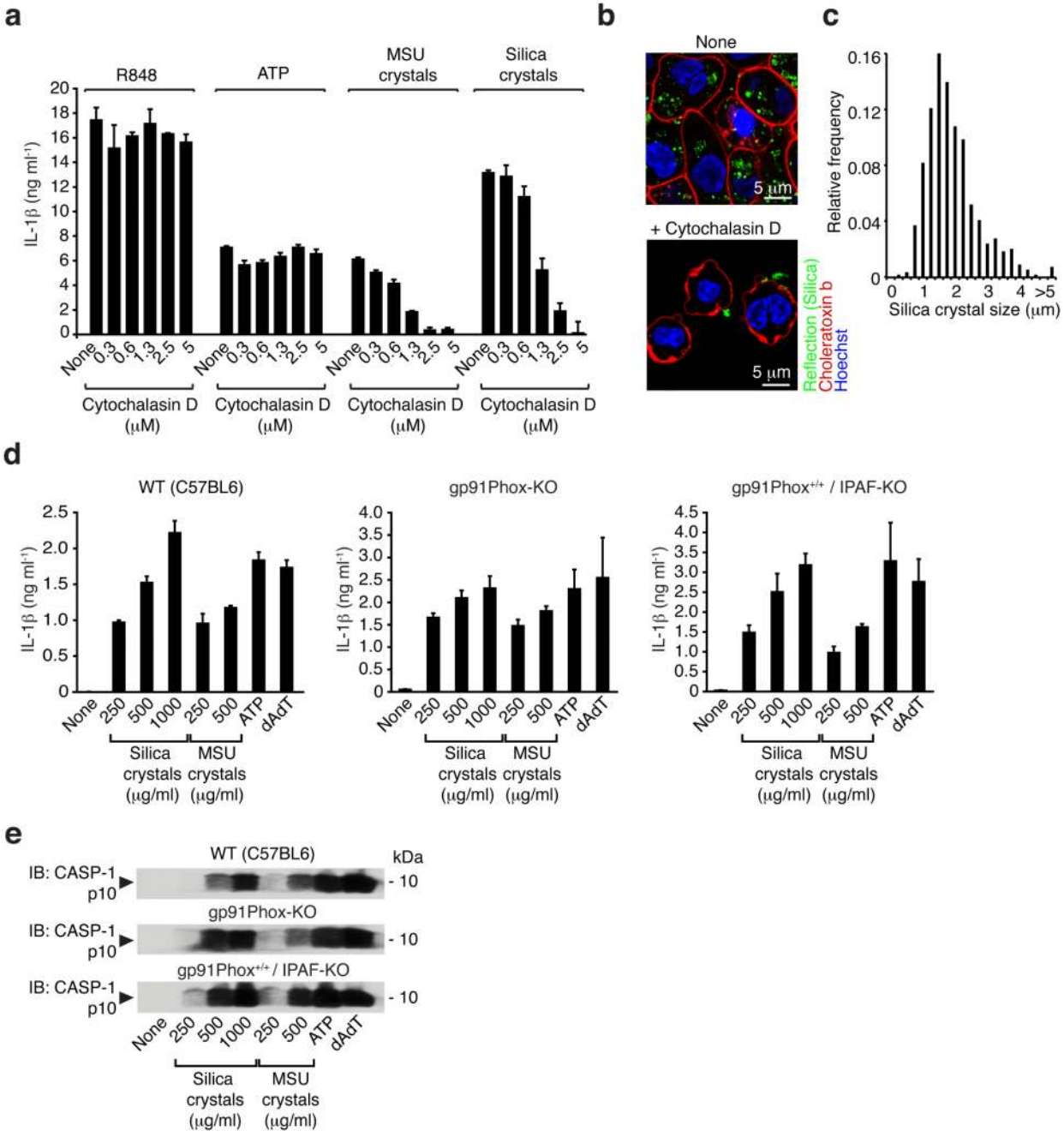

Fig. 4. Crystal uptake is required for inflammasome activation, whereas the phagosomal ROS system is not involved in crystal-mediated inflammasome activation

(a) Human LPS-primed PBMCs were treated with cytochalasin D in ascending doses and subsequently stimulated with silica crystals, MSU crystals or ATP. IL-1β release was measured by ELISA 6h after stimulation. Data from one representative experiment out of two are depicted. **(b)** B6-MCLs were stimulated for 2h with silica crystals in the presence or absence of cytochalasin D (2.5 μM). Cells were then membrane stained with fluorescent choleratoxin (red), nuclei stained with Hoechst dye (blue) and analyzed for crystal uptake (green) using confocal microscopy. **(c)** B6-MCLs were incubated with silica crystals as in **(b)** and phagocytosed silica crystals was analyzed for their length and the fractional

distribution of crystal sizes is shown from phagocytosed crystals of 10 representative cells. **(d and e)** Bone marrow-derived macrophages of wild-type mice, gp91Phox-deficient mice or IPAF-deficient mice (as a mixed background control) were primed with LPS for 3h and subsequently stimulated with either silica crystals, MSU crystals, ATP or transfected with dAdT. 6h after stimulation, supernatants were analyzed for IL-1β by ELISA **(d)** and assessed for activated caspase-1 by Western blot **(e)**. Data from one representative experiment out of two are depicted.

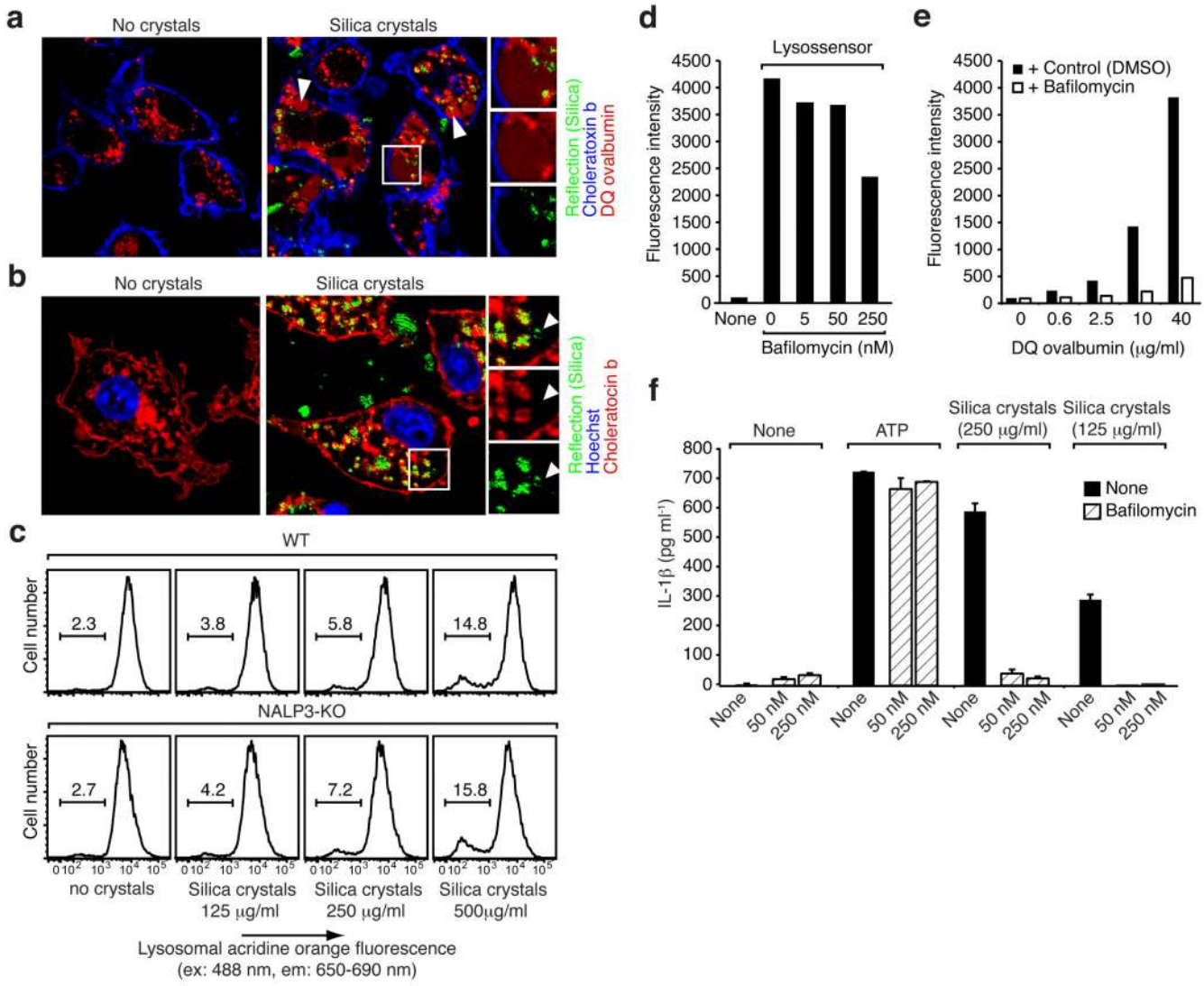

Fig. 5. Phagocytosis of crystals leads to lysosomal destabilization

(a) B6-MCLs were incubated with 10 μg/ml DQ-ovalbumin (red) alone or together with silica crystals (green) for 60 min, surface stained with fluorescent choleratoxin (blue) and analyzed by confocal microscopy. **(b)** B6-MCLs were incubated with silica crystals (green) for 60 min or left untreated, fixed, permeabilized (saponin 0.01%) and stained with fluorescent choleratoxin (red), Hoechst dye (blue) and analyzed by confocal microscopy. **(c)** B6-MCLs and NALP3-KO-MCLs were stained with acridine orange and subsequently treated with silica crystals as indicated. 3h after treatment cells were analyzed by flow cytometry for lysosomal acridine orange fluorescence. **(d)** B6-MCLs were treated with bafilomycin as indicated and stained with lysosensor green (1 μM) immediately prior to flow cytometry. **(e)** B6-MCLs were incubated with DQ-ovalbumin in the presence or absence of bafilomycin (250 nM) for 60 min and subjected to FACS analysis. **(f)** LPS-primed B6-MCLs were treated with bafilomycin or left untreated and subsequently stimulated with silica crystals or ATP. IL-1β release was measured by ELISA 6h after stimulation. Data from one representative experiment out of two are depicted.

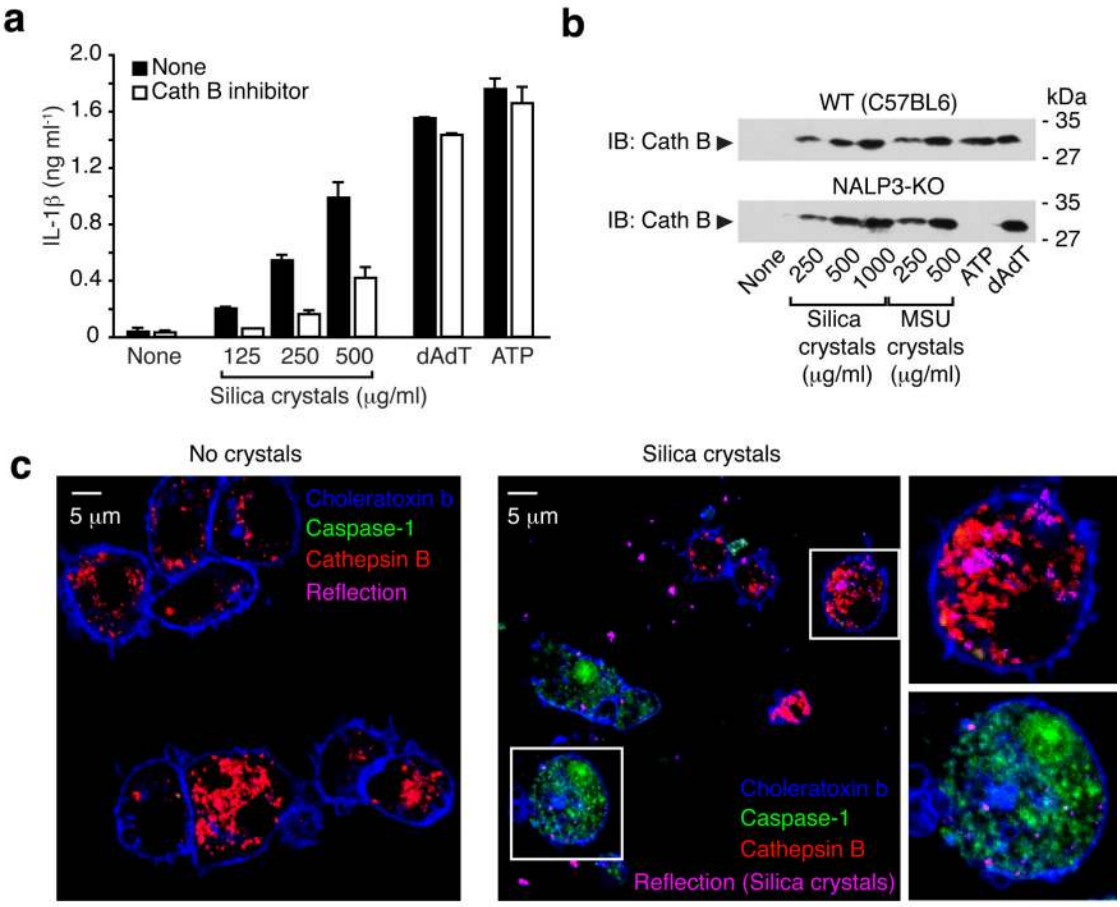

Fig. 6. Silica mediated IL-1b production is partially dependent on Cathepsin B

(a) LPS-primed B6-MCLs were treated with either cathepsin B inhibitor (CA-074-Me, 10 μM) or left untreated and subsequently stimulated with silica crystals, ATP or transfected with dAdT. IL-1β release was measured by ELISA 6h after stimulation. Data from one representative experiment out of two are depicted. **(b)** Bone marrow-derived macrophages of wild-type mice or NALP3-deficient mice were primed with LPS for 3h and subsequently stimulated with either silica crystals, MSU crystals, ATP or transfected with dAdT. 6h after stimulation, supernatants were analyzed for cathepsin B by Western blot. **(c)** B6-MCLs were incubated with silica crystals (pink) for 3 h or left untreated. Subsequently, cells were stained with fluorescent probes for activated caspase-1 (green) and activated cathepsin B (red) for one additional hour and then surface stained with fluorescent choleratoxin (blue) and analyzed by confocal microscopy.

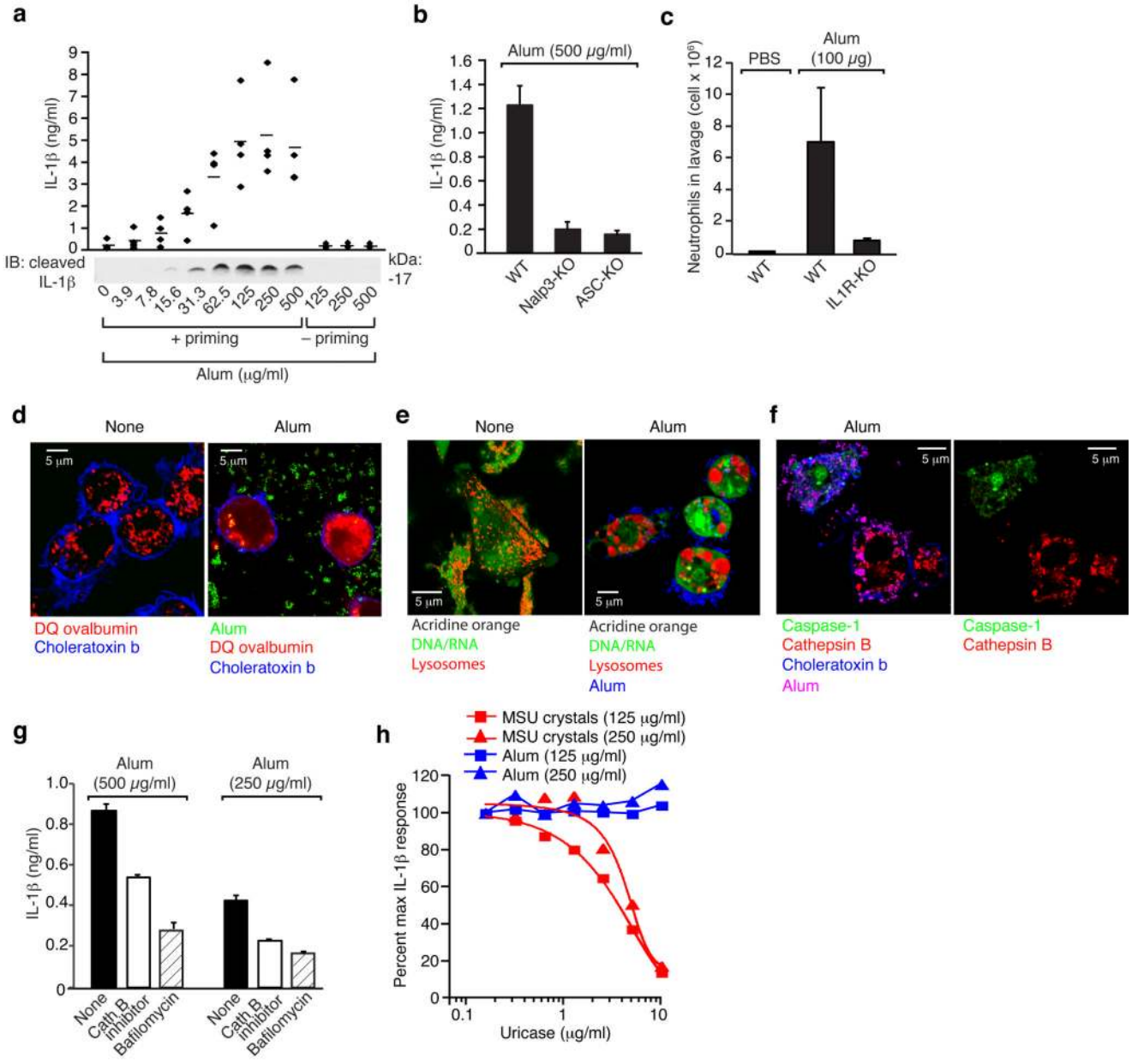

Fig. 7. Alum activates the NALP3 inflammasome via lysosomal destablization

(b) Human PBMCs were primed with LPS (25 pg/ml) or left untreated for 3h and subsequently stimulated with alum in ascending doses. After 6h, supernatants were assessed for IL-1β production by ELISA and Western blot. ELISA data of four independent donors are depicted (upper panel) and Western blot analysis of one representative donor is shown (lower panel). **(b)** Bone marrow-derived macrophages of wild-type mice, NALP3-deficient mice or ASC-deficient mice were primed with LPS for 3h and subsequently stimulated with alum (500 μg/ml) and supernatants were analyzed for IL-1β by ELISA. **(c)** Alum (100 μg) was injected i.p. into wild-type mice (n=5) or IL1R-deficient mice (n=5), whereas PBS served as a control in wild-type mice (n=3). 16–18h after injection neutrophil counts were monitored in the peritoneal lavage by FACS. **(d)** B6-MCLs were incubated with 10 μg/ml DQ-ovalbumin (red) alone or together with alum (green) for 60 min, surface stained with

fluorescent choleratoxin (blue) and analyzed by confocal microscopy. **(e)** B6-MCLs were stained with acridine orange and subsequently treated with alum (blue) as indicated. **(f)** B6-MCLs were incubated with alum (pink) for 3 h or left untreated. Subsequently, cells were stained with fluorescent probes for activated caspase-1 (green) and activated cathepsin B (red) for one additional hour and then surface stained with fluorescent choleratoxin (blue) and analyzed by confocal microscopy. **(g)** LPS-primed bone marrow-derived macrophages were treated with either cathepsin B inhibitor (CA-074-Me, 10 μM), bafilomycin (250 nM) or left untreated and subsequently stimulated with alum. IL-1β release was measured by ELISA 6h after stimulation. Data from one representative experiment out of two are depicted. **(h)** LPS-primed bone marrow-derived macrophages were treated with either alum or MSU in the presence of ascending doses of uricase. IL-1β release was measured by ELISA 6h after stimulation. Data were normalized to the condition without uricase.

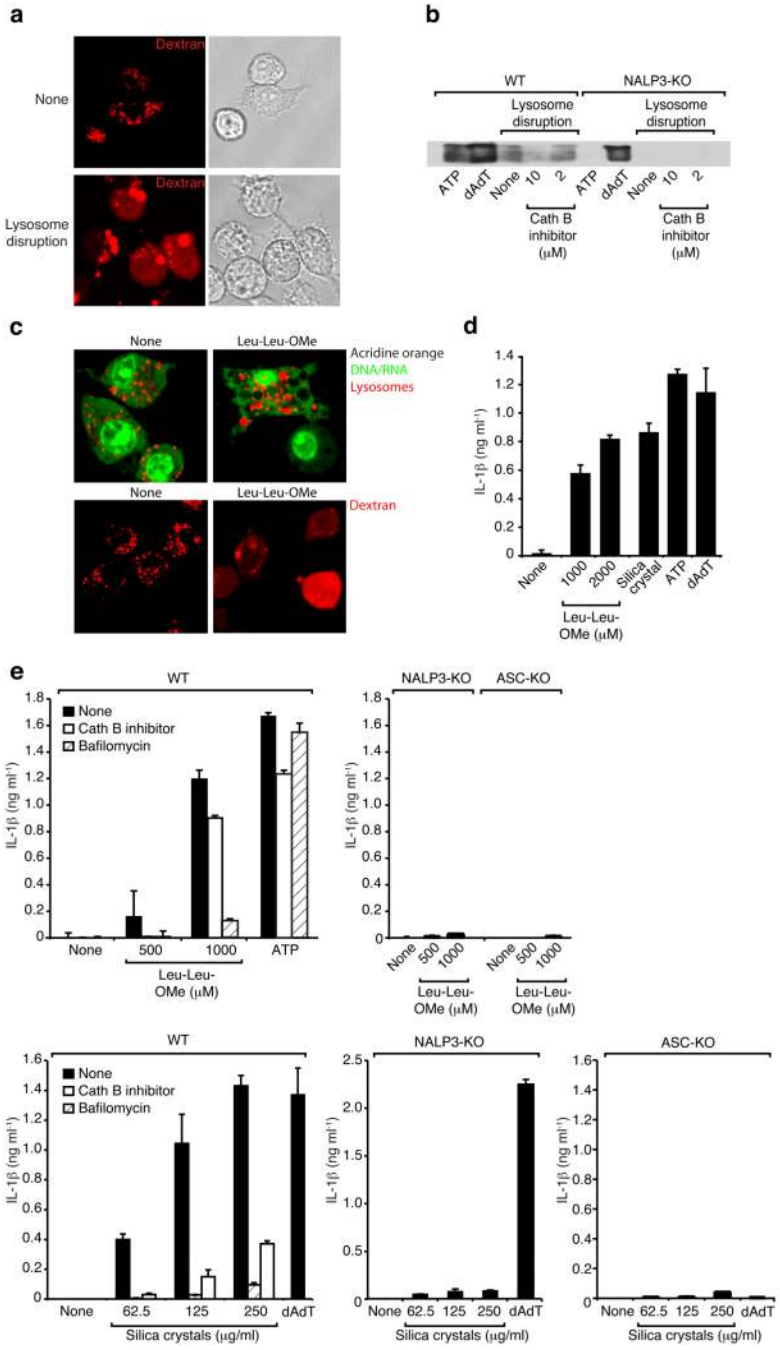

Fig. 8. Sterile lysosomal rupture activates the NALP3 inflammasome

(a) B6-MCLs were incubated in the presence of fluorescent dextran (red) for 30 min and were left untreated or were subsequently treated using hypertonic and hypotonic solutions (see Material and Methods) to induce lysosomal rupture. **(b)** Bone marrow-derived macrophages of wild-type mice or NALP3-deficient mice were treated as in (a) in the presence or absence of cathepsin B inhibitor (CA-074-Me, 10 or 2 μM). In addition, ATP or dAdT were used as controls. 5h after stimulation supernatants were analyzed for actiated caspase-1. Data from one experiment out of two are depicted. **(c)** B6-MCLs were labeled with acridine orange (upper panel) or incubated in the presence of fluorescent dextran (red; lower panel) and incubated with Leu-Leu-OMe (1000μM). 3h after incubation cells were

analyzed by confocal microscopy. **(d)** LPS-primed B6-MCLs were incubated with Leu-Leu-OMe (1000 or 2000 μM), silica crystals (250 μg/ml), ATP or dAdT. IL-1β release was measured by ELISA 6h after stimulation. Data from one representative experiment out of three is depicted. **(e)** Bone marrow-derived macrophages of wild-type mice, NALP3-deficient mice or ASC-deficient mice were primed with LPS and subsequently stimulated with Leu-Leu-OMe (500 or 1000 μM) and ATP in the presence or absence of cathepsin B inhibitor (CA-074-Me, 10 μM) or bafilomycin (250 nM) (upper panel). In addition cells were stimulated with silica crystals or dAdT in the presence or absence of cathepsin B inhibitor (CA-074-Me, 10 μM) or bafilomycin (250 nM) (lower panel).